ELSEVIER

Biochimica et Biophysica Acta 1276 (1996) 124–132

BBA Biochimica et Biophysica Acta

# A critical evaluation of in situ measurement of mitochondrial electrical potentials in single hepatocytes

Joachim J. Ubl [1], Jean-Yves Chatton, Shuhua Chen, Jörg W. Stucki *

*Institute of Pharmacology, University of Bern, Friedbühlstr. 49, CH-3010 Bern, Switzerland*

Received 15 January 1996; revised 22 April 1996; accepted 26 April 1996

**Abstract**

The range of applicability and the critical parameters involved in the assessment of mitochondrial electrical potential ($\Delta\Psi_{mit}$) using epifluorescence microscopy were evaluated based on both theoretical and experimental analysis. Rat hepatocytes loaded with the potential-dependent fluorescent dye rhodamine 123 exhibited the expected heterogeneity of fluorescence distribution with dark regions corresponding to the nucleus and bright regions corresponding to the mitochondria-rich cytosol. Calibration of the signal was performed by permeabilizing the cell membrane for monovalent cations using nystatin and gramicidin, and equilibrating the cell with a $K^+$-free bath solution. A voltage-clamp at defined $\Delta\Psi_{mit}$ was then achieved after addition of valinomycin in the presence of different $K^+$ concentrations in the bath. Theoretical analysis indicated that the ratio of fluorescence intensity measured in mitochondria-rich and mitochondria-poor regions of cell was related with $\Delta\Psi_{mit}$ and yielded quantitative estimates of electrical potential with an accuracy of 10–20 mV. The ratio tended to plateau at potentials more negative than −140 mV, showing a limitation of the technique. Manoeuvres such as imposing a heavy ATP demand or interfering with the mitochondrial respiration depolarized mitochondria, while $\Delta\Psi_{mit}$ was not altered in a measurable manner during $Ca^{2+}$ oscillations consecutive to $\alpha_1$-agonist stimulation.

*Keywords:* Mitochondrial potential; Rhodamine 123; Biguanide; Phenylephrine; $Ca^{2+}$ oscillation

## 1. Introduction

Mitochondria, the site of the cellular oxidative phosphorylation, supply ATP to the eukaryotic cells for their constant energy demand during functions such as biosynthesis, muscular contraction, ion and solute pumping. The mitochondrial respiratory chain gives rise to an electrochemical proton gradient across the inner mitochondrial membrane, which can be decomposed into its transmembrane electrical potential ($\Delta\Psi_{mit}$) component and its pH gradient component. The energy stored in this electrochemical gradient is the driving force for the proton flux through the $F_0F_1$ ATPase of the inner mitochondrial membrane and the resultant ATP synthesis [1]. As a consequence $\Delta\Psi_{mit}$ and the ATP demand are closely linked.

Measurement of $\Delta\Psi_{mit}$ in intact living cells has been made possible by fluorescence microscopy using lipophilic cationic dyes that accumulate electrophoretically in the strongly negatively-charged matrix of mitochondria [2]. This redistribution of dye was shown to be primarily governed by the Nernst Eq. [3]. Semi-quantitative $\Delta\Psi_{mit}$ measurements in hepatocytes, among the most metabolically active cells, has been previously performed in our laboratory [4] using this approach. This study showed that glycogenolytic stimuli by α-adrenergic agonists, while eliciting oscillations of the cytosolic free-calcium concentration, did not alter $\Delta\Psi_{mit}$ in a measurable manner. This raised the question of whether $\Delta\Psi_{mit}$ changes possibly existed during $Ca^{2+}$ oscillations but were not detectable by this method.

The present study was thus designed to critically evaluate microspectrofluorimetric measurements of $\Delta\Psi_{mit}$ using Nernstian dyes such as rhodamine 123 (Rh123) in order to delineate their applicability as well as their limits. This analysis was done through an extension of the theoretical

Abbreviations: Rh123, rhodamine 123; $\Delta\Psi_{mit}$, mitochondrial transmembrane electrical potential; $F_r$, fluorescence intensity from mitochondria-rich cytosolic area; $Fp$, fluorescence intensity from mitochondria-poor nucleus area; TMRE, tetramethyl rhodamine ester.

* Correspondence author. Fax: +41 31 3027230.

[1] Present address: Institut für Neurochemie, Otto-von-Guericke Universität, Leipzigerstr. 44, Haus 21, D-39120 Magdeburg, Germany.

0005-2728/96/$15.00 Published by Elsevier Science B.V.
*PII* S0005-2728(96)00067-9

basis developed previously in our laboratory [4] in conjunction with a newly developed in situ calibration procedure.

## 2. Material and methods

Rat hepatocytes were prepared as previously described [5]. Briefly, hepatocytes were isolated using an adaptation of the EDTA perfusion method [6] and then frozen in fetal bovine serum supplemented with 10% DMSO and kept in liquid nitrogen for up to 8 days. On experiment day, cells were thawed, washed and plated on collagen-coated glass coverslips and incubated at 37°C for 2 h in F12-bicarbonate medium containing 2% bovine serum albumin in 5% $CO_2$/95% air atmosphere. Unattached cells were then washed out before starting the experiment.

Normal perfusion solutions were either F12 culture medium (Sigma, Buchs, Switzerland) or Krebs-Henseleit containing (in mM) 120 NaCl, 5 KCl, 1 $MgSO_4$, 1 $KH_2PO_4$, 2.5 $CaCl_2$, 20 HEPES, 25 $NaHCO_3$, 20 glucose (pH 7.4). For calibrations, the cells were kept in a $K^+$-free solution (120 Na-gluconate, 25 NaCl, 1.8 $CaCl_2$, 0.8 $MgSO_4$, 8 HEPES, 10 glucose, pH 7.4). Calibration solutions, with $K^+$ concentration ranging from 0 to 25 mM, had a $Na^+$-gluconate concentration reduced by a corresponding amount.

The cells were incubated in the experimental solution containing 0.1 μM Rh123 alone or Rh123 plus 2–4 μM fura-2(AM) for 20 min at 37°C, and then washed with the same solution containing 0.1 μM Rh123. The coverslip was then mounted in a thermostated (35°C) perfusion chamber on the stage of an inverted epifluorescence microscope (Nikon, Tokyo, Japan) that allowed re-circulation or exchange of the bath medium. All bathing solutions used during the course of an experiment, including calibrations, contained 0.1 μM Rh123.

Excitation filters were rapidly exchanged by means of a motorized filter wheel (Lambda 10, Sutter Instruments, Novato, CA) placed in front of the Xenon lamp. Rh123 was excited at 480 nm and fura-2 was excited at 340 and 380 nm. For both dyes, a filter cube with 510 nm dichroic mirror and 520–560 nm band-pass filter was used. Cells were observed through a 40 × 1.3 N.A. objective lens (Nikon).

The emitted fluorescence was detected by a video camera equipped with image intensifier (KS-1380, Videoscope, Washington D.C.). The video image was acquired and digitized using an 8-bit frame grabber (Leutron, Glattbrugg, Switzerland). A computer program written in our department by Dr. B.F.X. Reber was used to control the image processor, the filter wheel and the image intensifier. During the experiment, several regions of interest in the field of view could be selected and integrated.

Nystatin, gramicidin, ouabain, antimycin A, rotenone and phenformin were purchased from Sigma (Buchs, Switzerland); Rh123 was from Molecular Probes (Eugene, OR) and metformin was a generous gift of Dr. N. Wiernsperger from Lipha, Lyon (France).

## 3. Theoretical analysis

### 3.1. Derivation of a modified Nernst equation

Cationic lipophilic dyes, such as Rh123, undergo redistribution between the extracellular milieu, the cytosol and intracellular organelles which is driven by the differences of membrane potentials. Because, in intact cells, the fluorescence signal arising from mitochondria is not accurately distinguishable from that of the cytosol using the currently available methods, the relative Rh123 concentration in the mitochondrial matrix and in the cytosol cannot be readily determined. As a consequence, the Nernst equation cannot be directly applied for calculating $\Delta\Psi_{mit}$.

We have developed an approach to determine the mitochondrial inner membrane potential using conventional epifluorescence microscopy. As depicted in Fig. 1, single rat hepatocytes loaded with Rh123 exhibit subcellular compartmentalization with bright regions corresponding to a high mitochondrial density ($F_r$) and a darker region of low mitochondrial density ($F_p$) corresponding to the nucleus. We consider two regions of interest as sections through the cell and assume that $F_r$ and $F_p$ are mixtures of

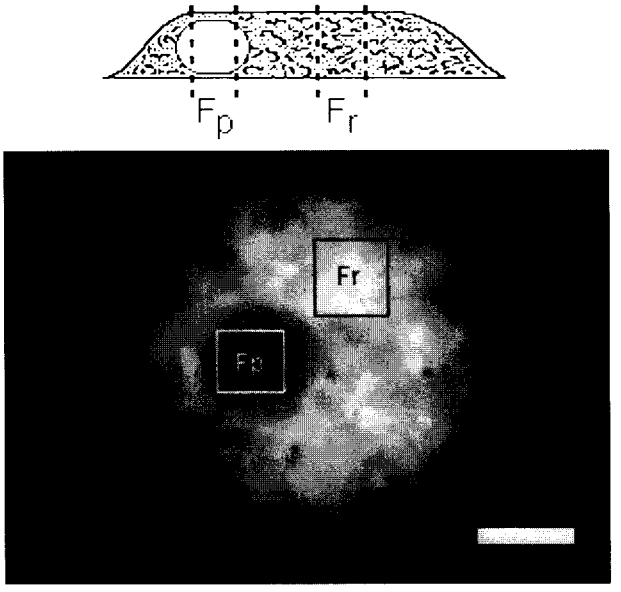


Fig. 1. Digitized video fluorescence image of a single rat hepatocyte loaded with Rh123. The fluorescence exhibits an non-uniform distribution within the cell. The two boxes represent the selected regions of interest in a mitochondria-rich ($F_r$) and a mitochondria-poor ($F_p$) region of the cell, corresponding to the cytosol and the nucleus, respectively (Scale bar = 5 μm). A schematic section through the two areas is shown above the fluorescence image.

the fluorescence intensities from pure mitochondria $f_m$ and pure cytosol $f_c$:

$$F_r = \alpha f_m + \beta f_c \quad (1)$$

$$F_p = \gamma f_m + \delta f_c \quad (2)$$

where $\alpha$, $\beta$, $\gamma$, and $\delta$ are unknown coefficients representing normalized volumes. Neglecting the contribution of the bound dye we further assume that

$$f_m = K_m c_m \quad (3)$$

$$f_c = K_c c_c \quad (4)$$

where $c_m$ and $c_c$ are the concentrations of the free dye in the mitochondrial matrix and the cytosol, respectively. The proportionality constants $K_m$ and $K_c$ stand for the fluorescence efficiencies of the dye in these compartments.

We consider now some geometrical properties of these sections. The sum of volumes $\alpha$ and $\beta$ reflects the total volume of the section $F_r$. Hence we can put

$$\alpha + \beta = 1 \quad (5)$$

$$\alpha/\beta = r \quad (6)$$

where $r$ is the ratio of the mitochondrial volume and the cytosolic volume in this section. The same goes for $F_p$, where we have

$$\gamma + \delta = 1 \quad (7)$$

$$\gamma/\delta = r/d \quad (8)$$

$d$ corresponds to the additional 'dilution' resulting from the nuclear volume which is essentially free of mitochondria. This parameter will be referred to as 'mitochondria dilution' in the following discussion. With these new parameters, the coefficients $\alpha$ through $\delta$ can now be expressed as follows:

$$\alpha = \frac{r}{1+r} \quad (9)$$

$$\beta = \frac{1}{1+r} \quad (10)$$

$$\gamma = \frac{r}{d+r} \quad (11)$$

$$\delta = \frac{d}{d+r} \quad (12)$$

Eq. (1) and Eq. (2) can be inverted to yield

$$\frac{f_m}{f_c} = \frac{\delta F_r - \beta F_p}{\alpha F_p - \gamma F_r} \quad (13)$$

For convenience, we define the variable

$$\varphi = \frac{d(1+r)}{d+r}\frac{F_r}{F_p} \quad (14)$$

Remembering the Nernst equations and using Eqs. (3) and (4) we have

$$\Delta\Psi = -\frac{RT}{zF}\ln\left(\frac{K_c f_m}{K_m f_c}\right) \quad (15)$$

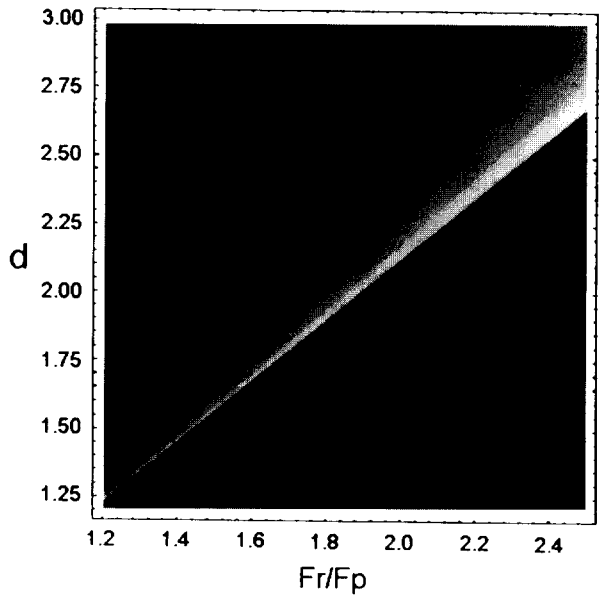


Fig. 2. Density plot of the function linking $\Delta\Psi_{mit}$, the 'mitochondrial dilution' $d$ and $F_r/F_p$. The magnitude of $\Delta\Psi_{mit}$ (−60 to −180 mV) is represented by 25 grey levels where white stands for −180 mV. As can be seen, for a given $d$ value, $\Delta\Psi_{mit}$ gradually increases to reach a maximum value after which the function yields imaginary values (black area).

By using Eqs. (9)–(14), we finally obtain

$$\frac{f_m}{f_c} = \frac{d(\varphi - 1)}{r(d - \varphi)} \quad (16)$$

and

$$\Delta\Psi = -\frac{RT}{zF}\ln\left(\frac{K_c}{K_m}\frac{d(\varphi - 1)}{r(d - \varphi)}\right) \quad (17)$$

Fig. 2 is a representation of Eq. (17) plotted against $d$ and $F_r/F_p$. The magnitude of $\Delta\Psi$ is expressed as 25 levels of grey extending from −60 mV (black) to −180 mV (white). The figure shows that, for a given $d$, $\Delta\Psi$ augments with increasing $F_r/F_p$ to reach a maximum after which the functions reaches imaginary values (black area). The figure also reveals that the curves tend to plateau at high values of $\Delta\Psi$. This points out to a major methodological limitation: accurate measurements of high $\Delta\Psi$ are possible only in cells with a high contrast between $F_r$ and $F_p$, i.e., with a high $d$ value. With conventional fluorescence microscopic techniques, the highest values of $d$ that we could measure were around 2.8.

### 3.2. Estimation of parameters

The parameters $K_m$ and $K_c$ can, in principle, be estimated from preparations of pure mitochondrial matrix and pure cytosol isolated by differential centrifugations of tissue homogenates. In liver, we obtained values of $K_c/K_m$ around 0.9. The parameters $d$ and $r$ can be estimated from

morphometric studies. $r$, the fraction of the mitochondrial matrix volume in the cytoplasm was estimated to be 0.12 for rat hepatocytes [7], while $d$, the density ratio of mitochondria in the mitochondria-rich versus mitochondria-poor regions, depends on the cell geometry and the optical performance of the microscope. It is therefore more practical to obtain these parameters from nonlinear fitting of the experimental data to Eq. (17) (see Section 4).

It is instructive to analyse some limits of Eq. (17). Meaningful values of the numerator and the denominator are bound by the inequalities

$$\varphi > 1 \tag{18}$$

$$d > \varphi \tag{19}$$

The first condition is always met since

$$F_r/F_p \geq 1 \tag{20}$$

However, inequality (Eq. (19)) imposes limitations on $d$ and $F_r/F_p$. Inserting Eq. (14) into Eq. (19) yields the limit

$$d = \left(\frac{F_r}{F_p}\right)_{max} (1 + r) - r \tag{21}$$

i.e., a linear relation between $(F_r/F_p)_{max}$ and $d$. This is a corollary to Eq. (17) and is actually a prediction of the model which can be tested experimentally. In Fig. 2 this separatrix can be seen as the line delimiting the white and the black areas. In Section 4 we considered values of $F_r/F_p$ measured at the very beginning of the experiment, $(F_r/F_p)_i$, as estimates of $(F_r/F_p)_{max}$. A plot of $d$ as a function of $(F_r/F_p)_i$ obtained from in different cells (Fig. 6) shows that the experimental data indeed fall on a straight line as predicted by Eq. (21). As a consequence, the strong dependence of $d$ on $(F_r/F_p)_i$ can be used as a good initial estimate for values of $d$.

### 3.3. Approximations of $\Delta\Psi$

It must be emphasized that the exact values of $\Delta\Psi$ can only be obtained after a fit of the data to Eq. (17). This needs a calibration of the individual cell under consideration at the beginning or at the end of the experiment. For practical reasons this is, however, not feasible, since the ionophores required for such calibrations cannot be washed out easily. Therefore we sought an approach that would yield semi-quantitative estimates of $\Delta\Psi$. A comparison of the parameters obtained from fits of a number of cells ($n = 27$) revealed that $K_c/K_m$ and $r$ show the least variations with mean values of 0.9 and 0.12, respectively. On the other hand, the parameter with the largest variation from cell to cell is $d$. As explained above, this parameter can, however, be estimated with a remarkable degree of accuracy by using the ratio $(F_r/F_p)_i$ at the beginning of the experiment.

Thus in order to rapidly estimate the $\Delta\Psi$'s in a semi-quantitative manner, we constructed a contour plot of Eq. (17) represented as a family of curves for different values of $\Delta\Psi$ (Fig. 3). The recipe for the determination of $\Delta\Psi$ with the help of this diagram goes as follows: (1) measure $(F_r/F_p)_i$ and approximate $d$ from Eq. (21) and the average value of $r$ determined previously. (2) Select a horizontal line corresponding to $d$. (3) Interpolate $\Delta\Psi$ at the intersection of this line with the measured $F_r/F_p$ after for instance a pharmacological intervention. One has to take into account that, as discussed above, this procedure is only accurate for values of $\Delta\Psi$ more positive than about $-140$ mV.

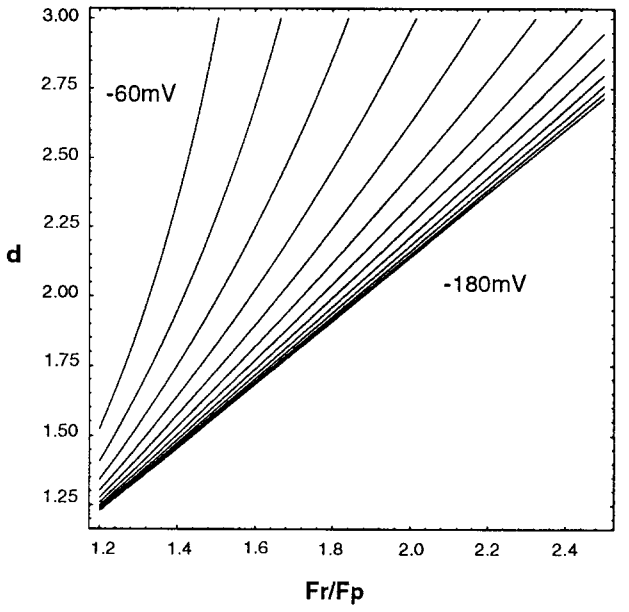


Fig. 3. Nomogram for an approximation of $\Delta\Psi_{mit}$. Knowing the 'mitochondrial dilution' $d$ (estimated using the initial value of $F_r/F_p$ and Eq. (21)), and the experimental $F_r/F_p$ values, a corresponding $\Delta\Psi_{mit}$ can be interpolated. A family of $\Delta\Psi_{mit}$ curves, corresponding to the data of Fig. 2, are represented in 10-mV steps extending from $-60$ mV through $-180$ mV.

## 4. Results

### 4.1. Measurement and calibration of $\Delta\Psi_{mit}$

Hepatocytes were loaded and then perfused throughout the experiment and calibration with Rh123 at a constant concentration of 0.1 μM. The fluorescence intensities in selected areas corresponding to $F_r$ and $F_p$ were continuously monitored. As schematized in Fig. 4, the calibration was started after exchanging the perfusion solution with a $K^+$-free calibration solution in the presence of the cation ionophores nystatin (10 μg/ml) and gramicidin D (5 μg/ml). This manoeuvre resulted in a replacement of the cytosolic $K^+$ by $Na^+$. To avoid an excessive ATP consumption due to the activation of the $Na^+/K^+$-ATPase, the pump inhibitor ouabain (1 mM) was added to the bath solution. Nystatin, gramicidin and ouabain were present

during the whole calibration procedure. After equilibration of concentrations (about 5 min), 2 μM valinomycin was added to selectively permeabilize the mitochondrial membrane for $K^+$ ions. In this situation, the electrical potential across the mitochondrial membrane was dictated primarily by the $K^+$ concentration on each side of the membrane. By assuming a $K^+$ concentration of 120 mM in the mitochondrial matrix space [8] and exchanging the bath medium to solutions with different $K^+$ concentrations, the measured fluorescence ratio $F_r/F_p$ could be related to the clamped $\Delta\Psi_{mit}$.

An original trace from such a calibration experiment is shown in Fig. 5A. After permeabilization of the plasma membrane with nystatin and gramicidin, the addition of 2 μM valinomycin (open arrowhead) caused no change of the fluorescence ratio $F_r/F_p$, indicating that the cytosolic $K^+$ was completely exchanged with $Na^+$ from the bath medium. An incremental increase in $K^+$ concentration (filled arrowheads) caused a stepwise decrease of $F_r/F_p$. The highest $K^+$ concentration that produced a consistent response was about 15 mM. As seen in the experiment presented in Fig. 5A, superfusion of 25 mM $K^+$ gave rise to an incomplete deflection of $F_r/F_p$ that was not used in the later calculations. As depicted in the last part of the plot, going back to low $K^+$ concentrations in the bath partly reversed $F_r/F_p$. As observed in many such experiments, the addition of ionophores caused a slow decline of $F_r/F_p$ independent of the addition of $K^+$. While this phenomenon did not seem to be the consequence of a gradual depletion of $K^+$ from the mitochondrial matrix, it could be the result of an undefined effect of the ionophores on the fluorescent signal.

The relationship between the measured fluorescence ratio, $F_r/F_p$, and the calculated $K^+$ diffusion potential, $\Delta\Psi_{mit}$, of the same experiment is presented in Fig. 5B. For

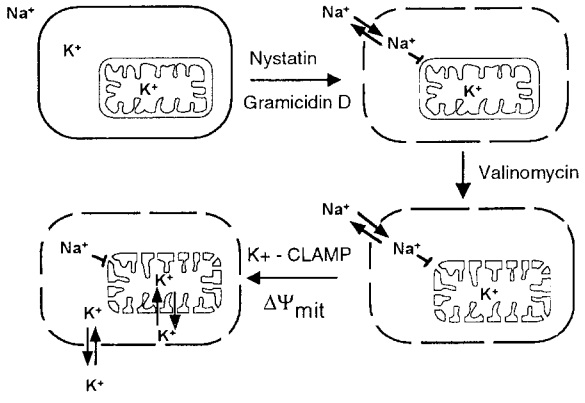


Fig. 4. Scheme of the calibration procedure. Addition of nystatin and gramicidin D in the absence of $K^+$ permeabilizes the cell membrane to cations and allows replacement of cytosolic $K^+$ by $Na^+$. Subsequent application of the $K^+$-ionophore valinomycin, to permeabilize the mitochondrial membranes, and superfusion of cells with solutions containing different $K^+$ concentrations enable the clamping of $\Delta\Psi_{mit}$ to known values used for calibration of the fluorescent signal.

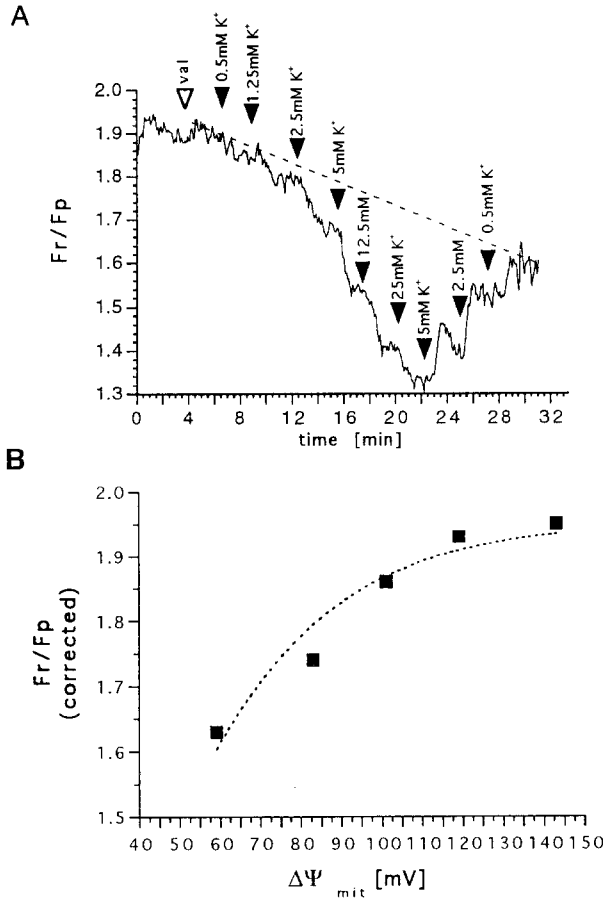


Fig. 5. Calibration of Rh123 signals. (A) Original calibration trace, starting after permeabilization of the plasma membrane for monovalent cations and replacement of cytosolic $K^+$. The addition of 1μM valinomycin (open arrowhead) caused no change in $F_r/F_p$. Increasing the $K^+$ concentration, as indicated by the filled arrowheads, caused a stepwise decrease of $F_r/F_p$ that was partly reversible. The dotted line indicates the general declining trend associated with the use of ionophores, that was removed for the fit of parameters. (B) Relationship between the measured ratio ($F_r/F_p$, from panel A) after subtraction of drift and the calculated $K^+$ diffusion potential ($\Delta\Psi_{mit}$, mV). The dotted line is a fit of the modified Nernst Eq. (14) and Eq. (17). These plots are representative of 9 different experiments.

this plot, the slope of the declining trend, indicated in panel A by the dotted line, was subtracted from the measured $F_r/F_p$. The relationship between the corrected $F_r/F_p$ and the calculated $\Delta\Psi_{mit}$ could well fit the modified Nernst equation (Eq. (14) and (17)) as indicated by the dotted line. For the fit, the ratio of the mitochondrial matrix to the cytosolic volume, $r$, was assumed to be 0.12 [7] while the 'mitochondria dilution', $d$, and the ratio of the fluorescence efficiency, $K_c/K_m$, were used as the free parameters to be estimated using the nonlinear fitting routine contained in the KaleidaGraph software package (Synergy Software, Reading, PA). From 9 different calibration experiments we obtained for $K_c/K_m$ a mean value of 0.89 ± 0.09 (S.E.M.) and a mean $d$ value of 2.10 ± 0.09.

As expected from the theory $d$ markedly depended on

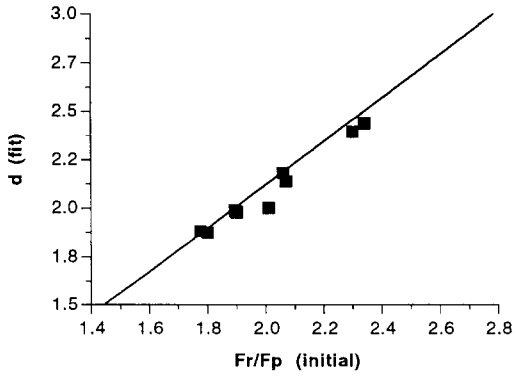


Fig. 6. Correlation between $F_r/F_p$ measured at the beginning of the calibration experiments and the 'mitochondria dilution' parameter $d$. Values of $d$ were obtained by fitting Eq. (14) and Eq. (17). The linear relationship (solid line) could be predicted by Eq. (21).

the geometry of the cell. However, as shown in Fig. 6, a linear relationship was found between the calculated $d$ value and the $F_r/F_p$ value measured right after the start of the experiment. This is in agreement with the theory as the Eq. (21) relating $F_r/F_p$ and $d$ nicely fitted the observations. This enabled the estimation of the unknown parameter $d$ from the measured ratio $F_r/F_p$ at the beginning of each experiment and, with the help of the nomogram shown in Fig. 3, the estimation of the corresponding mitochondrial potential. Similar results were obtained by using tetramethyl rhodamine ester (TMRE) instead of Rh123 ($n = 3$, results not shown).

Rh123 curves (see, e.g., Fig. 7) generally exhibit a substantial noise level and, in many experiments, some periodicity of signal fluctuations seemed to be present. This led us to investigate whether these fluctuations were only stochastic events. Steady-state recordings of $F_r/F_p$ signal were performed over up to 2-h periods with different data acquisition rates. Recordings were analyzed using Fourier power spectrum as well as autocorrelation methods according to Ref. [9]. Although some degree of autocorrelation, having the shape of a sinusoidal fluctuation of $\Delta\Psi_{mit}$ with a period in the order 10 min, was present in a few experiments, no consistent rhythmic fluctuations of significant amplitude were observed in hepatocytes ($n = 17$, data not shown).

### 4.2. $\Delta\Psi$ and ATP utilization

The energy stored in the electrochemical gradient across the inner mitochondrial membrane, i.e., $\Delta\Psi_{mit}$ and $H^+$ gradient, drives the synthesis of ATP by the $F_0F_1$ ATPase. This led us to postulate that an intensive ATP utilization should cause a drop of $\Delta\Psi_{mit}$, and a detectable alteration of the Rh123 fluorescence.

To test this hypothesis, a high ATP demand was imposed on the cells by means of a maximal stimulation of the $Na^+/K^+$-ATPase. This was achieved by increasing the cation permeability of the plasma membrane using the antibiotic nystatin in a $Na^+$-containing bathing medium. Fig. 7 shows that the addition of 50 μg/ml nystatin induced a drop in $F_r/F_p$ and therefore in $\Delta\Psi_{mit}$. The maximal stimulation of the $Na^+/K^+$-pump caused $\Delta\Psi_{mit}$ to decrease by 33.2 ± 5.5 mV. As shown in Fig. 7, in 11 different experiments, application of 1 mM ouabain, a specific inhibitor of the $Na^+/K^+$-ATPase, reversed (in 4 experiments) or interrupted (in 6 experiments) the nystatin-induced decrease of $\Delta\Psi_{mit}$. Ouabain was ineffective in only one experiment. The effects of ouabain are consistent with a reduction of the pump activity and its associated ATP consumption. These experiments confirmed that the ATP demand and $\Delta\Psi_{mit}$ are indeed linked, and that measurement of $\Delta\Psi_{mit}$ in a living cell can indirectly serve as a measurement of ATP consumption.

### 4.3. Effect of phenylephrine and biguanides on $\Delta\Psi_{mit}$

Stimulation of hepatocytes with $\alpha_1$-adrenergic agonists such as phenylephrine, triggers sustained oscillations of the cytosolic free calcium concentration [10,11]. The next experiments were performed to test whether such oscillations could induce, or be associated with changes in $\Delta\Psi_{mit}$. Hepatocytes loaded simultaneously with the calcium-sensitive probe fura-2 and Rh123 were sequentially illuminated at 340, 380 and 480 nm. As depicted in Fig. 8, phenylephrine induced $Ca^{2+}$ oscillations, as seen on the fura-2 trace, the frequency of which was dependent on the dose of phenylephrine. In 18 experiments, Rh123 did not exhibit a corresponding oscillating behavior and was largely unaffected by phenylephrine. In a few experiments (data not shown), overstimulation by phenylephrine induced a moderate decline in $F_r/F_p$. Addition of the respiratory chain inhibitor antimycin A stopped $Ca^{2+}$ oscillations and induced a large and sudden decrease of $F_r/F_p$.

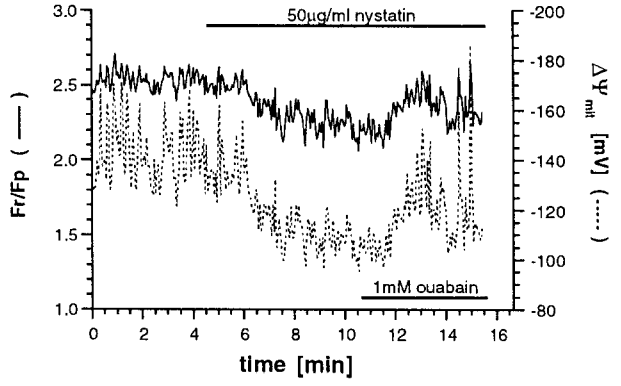


Fig. 7. Effect of high energy demand on $\Delta\Psi_{mit}$ in single rat hepatocytes. Single rat hepatocytes were loaded with 0.1 μM Rh123 and the ratio $F_r/F_p$ was continuously monitored (solid line). The time course of the calculated $\Delta\Psi_{mit}$ is indicated in the same plot (dotted line). Addition of 50 μg/ml nystatin in the bath solution caused a drop of $F_r/F_p$ and $\Delta\Psi_{mit}$. Subsequent addition of 1mM ouabain almost completely restored the initial values. Similar results were obtained in 4 independent experiments.

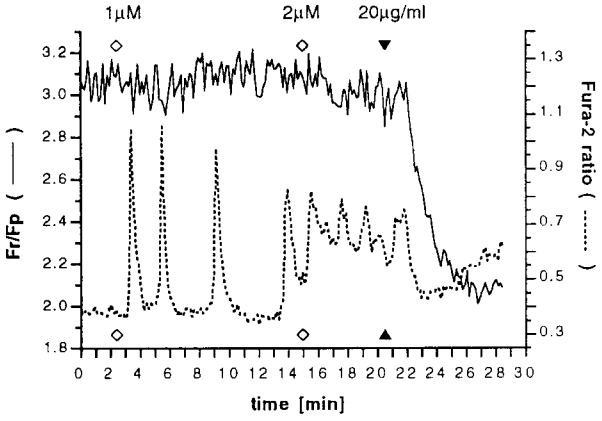


Fig. 8. Cytosolic $Ca^{2+}$ oscillations and Rh123 fluorescence ratio. Hepatocytes loaded with fura-2 (dotted line, right ordinate) and Rh123 (solid line, left ordinate) were sequentially stimulated with 1.0 and 2.0 μM phenylephrine (open diamonds). Antimycin A addition (20 μg/ml) is indicated by the closed triangles. The cytosolic free $Ca^{2+}$ concentration changes are proportional with the 340/380 nm fluorescence ratio of fura-2 and are presented in arbitrary units.

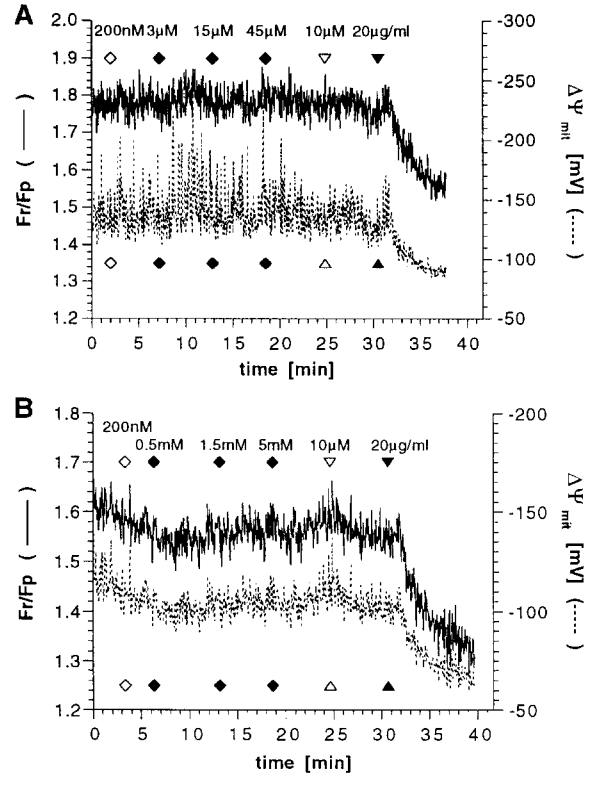


Fig. 9. Effects of the biguanides phenformin (panel **A**) and metformin (panel **B**) on $\Delta\Psi_{mit}$. The time course of $F_r/F_p$ (solid line) and the corresponding $\Delta\Psi_{mit}$ (dotted line) are presented in typical experiments. The successive additions of phenylephrine (open diamond), biguanides (closed diamonds), rotenone (open triangle) and antimycin A (closed triangle) with the respective concentrations are indicated on the graph. Only the respiratory chain inhibitor antimycin A caused a significant decrease of $F_r/F_p$ and $\Delta\Psi_{mit}$. The presented plots are representative of a total of 9 different experiments.

We recently demonstrated that antihyperglycaemic biguanides, such as phenformin and metformin, inhibited the α-agonists-induced calcium oscillations by a direct negative interference with the inositol 1,4,5-trisphosphate-sensitive calcium channel of the intracellular calcium stores [5]. Another action of biguanides is the inhibition of gluconeogenesis with the side-effect of increased circulating lactic acid [12]. It has been postulated that this effect was the consequence of a stimulation of the pyruvate kinase activity by biguanides by a mechanism involving a decrease in the cellular ATP production [13] eventually also due to an inhibition of the respiratory chain.

The anti-diabetic biguanides metformin and phenformin, were added on cells stimulated with phenylephrine (Fig. 9). Application of up to 45 μM phenformin ($n = 9$) or up to 5 mM metformin ($n = 9$), about 500-fold the therapeutic dose [14] did not influence $\Delta\Psi_{mit}$. As a control, at the end of these experiments the respiratory chain inhibitors rotenone (10 μM) and antimycin A (20 μg/ml) were added to cause the collapse of $\Delta\Psi_{mit}$. As Fig. 9 shows, the site I inhibitor rotenone did not induce a change in the fluorescence ratio, whereas the site II inhibitor antimycin A resulted in the expected decrease of $F_r/F_p$.

## 5. Discussion

The present study shows that $\Delta\Psi_{mit}$ can indeed be measured in single intact rat hepatocytes. Ratioing a measured region and a reference region and applying an in situ calibration protocol allowed us a semi-quantitative assessment of $\Delta\Psi_{mit}$, which showed that hepatocytes can handle moderate ATP demands, such as those occurring during $Ca^{2+}$ oscillations, without significant changes in the $\Delta\Psi_{mit}$.

Assessment of mitochondrial membrane potential using fluorescent lipophilic cations, has been described since the early 1970s [15]. These dyes redistribute across cellular membranes (plasma and inner mitochondrial membrane) according to the potential differences between each side of the membrane. Thus, in theory, the membrane electrical potential can be deduced from measurements of the dye concentration on each side of the membrane by using the Nernst Eq. [3]. Qualitative changes in mitochondrial membrane potential have been observed in intact living cells [3,16], while quantitative measurements have so far been performed only with isolated mitochondria [8] or mitochondria of digitonin-permeabilized cells [17]. The main obstacle for the quantitative application of this method to living cells is that the dye first equilibrates between the bath and the cytosol, driven by the cell membrane electrical potential, and then between the cytosol and the mitochondrial matrix according to $\Delta\Psi_{mit}$. Thus, in the absence of simultaneous determination of dye concentration in the cytosol and in the matrix, $\Delta\Psi_{mit}$ cannot be accurately estimated. Using digital video imaging microscopy Farkas et al. [18] simultaneously monitored the fluorescence inten-

sities in areas corresponding to the intramitochondrial and intracellular space but were able to follow only relative variations of potential. Conventional fluorescence microscopes, as well as confocal microscopes do not generally allow accurate distinction between the fluorescence originating from the mitochondria or from the cytosol ([18] and personal observations), mainly because of the small size and intrinsic motility of the mitochondria. Loew et al. [19,20] succeeded in measuring $\Delta\Psi_{mit}$ of single mitochondria in the neurites of neuroblastoma cells where, because of the spatial confinement imposed by the small cylindrical shape of neurites, movement of mitochondria and out-of-focus signal from neighboring mitochondria were minimal. Such conditions are not found in hepatocytes that possess a compact cell body with a high density of mitochondria. A different approach has therefore to be applied.

The cell nucleus excludes mitochondria and possesses large pores in its membrane, allowing quasi-electrical and chemical equilibrium with the cytosol [18]. The nuclear milieu should therefore adequately reflect the cytosolic Rh123 concentration. In the present study, we proposed to estimate the cytosolic Rh123 concentration by measuring its fluorescence in the nuclear region. Both theoretical and experimental analyses were used to define the range of applicability of this approach. Firstly, Eq. (16) and (17) show that the range of measurable $\Delta\Psi_{mit}$ strongly depends on the reference region that should ideally be devoid of any mitochondrial signal. This has direct influence on the parameter $d$, which will therefore depend on the cell geometry (e.g., thickness of cell vs. nucleus) as well as on the optical resolution of the microscope. This limitation, recognized at the level of the theoretical analysis, was confirmed by the calibration experiments that showed a flattening of the curve at potential more negative than $-140$ mV. Typical values of $d$ were found in the range 1.8 to 2.8, which sets the theoretical limits of measurable potentials in the range from zero to about $-160$ mV. Another consequence is that $\Delta\Psi_{mit}$ might be underestimated in cells that exhibit small $d$ values. This problem can be partly overcome by selecting flat cells where the nucleus occupies most of the cell thickness with little cytosol left above and under it. Achieving higher spatial resolution by using confocal fluorescence microscopy or digital deconvolutions [21] should also increase the range of measurable $\Delta\Psi_{mit}$. Another difficulty stems from the limited dynamic range of the camera which does not allow accurate simultaneous measurements in the dark nuclear region and the very bright mitochondria-rich cytosol. This unfortunately happens in cells having a high $d$ or in confocal fluorescence microscopy (unpublished observations) and therefore also limits the range of measurable electrical potential. Technical solutions such as double exposure using two intensifier gain settings or two illumination intensities, could be implemented to circumvent this problem, but would reduce the time resolution. In its present state of development, this method let us follow changes in $\Delta\Psi_{mit}$ with an accuracy of 10–20 mV in the normal range of mitochondrial potential.

We tested if the method was able to detect changes in $\Delta\Psi_{mit}$ consecutive to an ATP demand [22]. The rationale was that a substantial ATP utilization by the cell should force the mitochondria to operate at an increased rate to maintain the cellular ATP level, thereby causing a reduction in $\Delta\Psi_{mit}$. After an activation of the $Na^+/K^+$-ATPase caused by an increase in the cytosolic $Na^+$ concentration, a drop in the $F_r/F_p$ signal ratio was observed and corresponded to a $\Delta\Psi_{mit}$ decrease of about 33 mV. This effect was truly associated with the activity of the pump since application of ouabain reversed $\Delta\Psi_{mit}$ to its initial value. This demonstrated the measurable effect of unusually high ATP consumption on $\Delta\Psi_{mit}$. The question remains whether such an effect also existed during normal cellular functions requiring a more moderate ATP demand.

Hepatocytes respond to α-adrenergic agonist stimulation by oscillation of cytosolic free $Ca^{2+}$ [10]. The reason for preferring an oscillating behavior over a mere increase in $Ca^{2+}$ is still a matter of debate. One possibility is the energetic advantage of oscillations compared with simple monophasic $Ca^{2+}$ rise [23]. This model predicts that the energy needed to produce $Ca^{2+}$ oscillations is substantially smaller than a simple monophasic $Ca^{2+}$ increase. A previous report from our laboratory [4] showed that hepatocytes failed to demonstrate measurable variations in mitochondrial potential during $Ca^{2+}$ oscillations. We decided to re-investigate the question using our refined technique and analysis method. Confirming our earlier results, $\Delta\Psi_{mit}$ did not vary in a measurable manner during $Ca^{2+}$ oscillations. This result indicates that the energy expense of oscillations is probably moderate and is handled by the mitochondria without alteration of their proton-motive force. Loew et al. [20], investigating single mitochondria in the neurites of neuroblastoma cells using TMRE, showed that, during a $Ca^{2+}$-spike induced by bradykinin, $\Delta\Psi_{mit}$ transiently depolarized by about 10 mV, i.e., from $-158$ mV to $-147$ mV. The authors of this study hypothesized that the observed depolarization of mitochondria was consecutive to an increased energy demand rather than to the electrogenic flux of $Ca^{2+}$ into the mitochondria that would diminish their electrical potential. Indeed, the electrogenic $Ca^{2+}$ uniporter of the mitochondrial membrane has an activation constant much higher than the resting $Ca^{2+}$ (1–189 μM) and takes several seconds to get activated [24]. Therefore, a $Ca^{2+}$ spike that reaches the micromolar range only very briefly will induce only a limited entry of $Ca^{2+}$ that is unlikely to substantially affect $\Delta\Psi_{mit}$.

If $\Delta\Psi_{mit}$ changes of small magnitude such as described by Loew et al. [20] occur in hepatocytes during $Ca^{2+}$ oscillations, they would probably remain undetected, due to the limited sensitivity of the method. On the other hand, it is conceivable that, due to the higher density of mitochondria of hepatocytes compared to neurites of neuroblas-

toma cells, the energy load of a $Ca^{2+}$ spike per mitochondrion is much lower in hepatocytes.

The glucose-lowering agents phenformin and metformin have been used in the treatment of non-insulin-dependent diabetes mellitus. Their mechanism of action, although still uncertain, is associated with an inhibition of gluconeogenesis without stimulation of insulin secretion [25]. In rat hepatocytes, biguanides have recently been shown to interrupt $Ca^{2+}$ oscillations induced after glycogenolytic stimulus by phenylephrine, by direct negative interference with the $IP_3$-modulated $Ca^{2+}$ channel of the intracellular stores [5]. In the present study, application of biguanides during stimulation by the α-agonist phenylephrine had no effect on $\Delta\Psi_{mit}$. A side effect of biguanides is the occurrence of lactic acidosis, thought to be consecutive to an increase in anaerobic glycolysis [12]. Metformin was linked with redox-state changes in hepatocytes [13] that were accompanied with a decrease in the cellular ATP concentration. Our study shows that neither phenformin nor metformin, at concentrations up to 5 mM, produced detectable alterations of $\Delta\Psi_{mit}$. Therefore these experiments indicate that the lactic acidosis observed in some patients is probably not the consequence of a direct block of the respiratory chain by biguanides.

In summary, the present study evaluated measurements of $\Delta\Psi_{mit}$ in single intact hepatocytes using Nernstian dyes. Accurate $\Delta\Psi_{mit}$ measurements depend primarily on the ability to estimate the fluorescence intensity in the cytosol and the matrix, which limits our method to $\Delta\Psi_{mit}$ more positive than about $-140$ mV when conventional fluorescence microscopy is to be used. The study also showed that $\Delta\Psi_{mit}$ in intact cells is not influenced by small magnitude changes in ATP during normal cellular functions and only major ATP expense can significantly diminish it.

## Acknowledgements

This work was supported by the Swiss National Science Foundation (Grant 31-39605.93) and by Lipha, Lyon. We thank Dr. N. Wiernsperger for helpful discussion and Dr. H. Liu for her help during this study.

## References

[1] Mitchell, P. (1979) Science 206, 1148–1159.
[2] Chen, L.B. (1988) Annu. Rev. Cell Biol. 4, 155–181.
[3] Ehrenberg, B., Montana, V., Wei, M.-D., Wuskell, J.P. and Loew, L.M. (1988) Biophys. J. 53, 785–794.
[4] Reber, B.F.X., Somogyi, R. and Stucki, J.W. (1990) Biochim. Biophys. Acta 1018, 190–193.
[5] Ubl, J.J., Chen, S. and Stucki, J.W. (1994) Biochem. J. 304, 561–567.
[6] Meredith, M.J. (1988) Cell Biol. Toxicol. 4, 405–425.
[7] Hoek, J.B., Nicholls, D.G. and Williamson, J.R. (1980) J. Biol. Chem. 255, 1458–1464.
[8] Emaus, R.K., Grunwald, R. and Lemasters, J.J. (1986) Biochim. Biophys. Acta 850, 436–448.
[9] Bendat, J.S. and Piersol, A.G. (1971) Random Data: Analysis and Measurement Procedures. Wiley-Interscience, New York.
[10] Rooney, T.A., Sass, E.J. and Thomas, A.P. (1989) J. Biol. Chem. 264, 17131–17141.
[11] Somogyi, R. and Stucki, J.W. (1991) J. Biol. Chem. 266, 11068–11077.
[12] Bailey, C.J., Wilcock, C. and Day, C. (1992) Br. J. Pharmacol. 105, 1009–1013.
[13] Argaud, D., Roth, H., Wiernsperger, N. and Leverve, X.M. (1993) Eur. J. Biochem. 213, 1341–1348.
[14] Wollen, N. and Bailey, C.J. (1988) Biochem. Pharmacol. 37, 4353–4358.
[15] Loew, L.M. (1993) in Fluorescent and Luminescent Probes for Biological Activity (Mason, W.T., Ed.), pp. 150–160, Academic Press, London.
[16] Johnson, L.V., Walsh, M.L., Bockus, B.J. and Chen, L.B. (1981) J. Cell Biol. 88, 526–535.
[17] Vercesi, A.E., Bernardes, C.F., Hoffmann, M.E., Gadelha, F.R. and Docampo, R. (1991) J. Biol. Chem. 266, 14431–14434.
[18] Farkas, D.L., Wei, M.-D., Febbroriello, P., Carson, J.H. and Loew, L.M. (1989) Biophys. J. 56, 1053–1069.
[19] Loew, L.M., Tuft, R.A., Carrington, W. and Fay, F.S. (1993) Biophys. J. 65, 2396–2407.
[20] Loew, L.M., Carrington, W., Tuft, R.A. and Fay, F.S. (1994) Proc. Natl. Acad. Sci. USA 91, 12579–12583.
[21] Agard, D.A. and Sedat, J.W. (1983) Nature 302, 676–681.
[22] Berry, M.N., Gregory, R.B., Grivell, A.R., Henly, D.C., Nobes, C.D., Phillips, J.W. and Wallace, P.G. (1988) Biochim. Biophys. Acta 936, 294–306.
[23] Stucki, J.W. (1995) in Calcium Waves, Gradients and Oscillations. Ciba Foundation Symposium 188 (Bock, G.R. and Ackrill, K., Eds.), pp. 267–268, Wiley, Chichester.
[24] Gunter, T.E. and Pfeiffer, D.R. (1990) Am. J. Physiol. 258, C755–C786.
[25] Bailey, C.J. (1992) Diabetes Care 15, 755–772.